Fluorescence Cross Correlation Spectroscopy to Study Hemodynamics

Bachelor thesis

by

AMAIA VILLA ABAUNZA

Supervisor: prof. Maddalena Collini

Co-tutor: Margaux Bouzin

Home supervisor: Jon Urrestilla Urizabal

Università degli studio di Milano Bicocca – Physics Department

Academic year 2014 – 2015

Ai miei aimici dell‘unitá di biofisica

Contents

Chapter 1

Introduction

In the recent years a series of optical correlation techniques have been developed in order to be able to measure flow velocity with high spatial resolution while being non-invasive in order to be employed in-vivo on biological organisms.

The technique employed in my thesis work, scanning laser image correlation (SLIC), is a powerful approach for the detection of flow motions because it overcomes some limitations of the classical spectroscopy techniques. SLIC method consists in repeated laser scans over a linear pattern and on the cross correlation of the signal emitted by the excited fluorophores in different positions along the scan line. Therefore, the resulting measurements for flow velocity are really accurate.

One of the advantages of the SLIC is that it can be applied to the study of flow dynamics in living organisms, such as the zebrafish embryo considered in the thesis work. The zebrafish circulatory system has been observed after having injected different concentrations of morpholino, a substance that weakens the muscles, including the heart, and therefore alters the blood flow speed. The analysis has been done for a healthy and unhealthy zebrafish embryos and the obtained results have been compared (this is explained in chapter 4). In all the observed unhealthy embryos it has been found that the blood speed does substantially decrease in the main vessels. Apart from that, the variation of the speed for different positions of the vessels has been studied; in the regions near the heart the blood flow speed is higher for the case of the systolic phase, while in the diastolic phase and the vein this trend has not been observed.

Chapter 2

Theoretical Principles and Experimental Setup

2.1 Fluorescence

2.1.1 General features

In figure 2.1 the Jablonsky diagram showing the electronic and vibrational energy levels of a fluorophore (a fluorescent molecule) is reported. The separation between electronic levels is of the order of eV, while that between the vibrational levels is tens of meV. At room temperature, the molecule is typically in the lowest electronic level. In fact, at this temperature the thermal energy (κ_BT) is too low to produce thermally excited population.

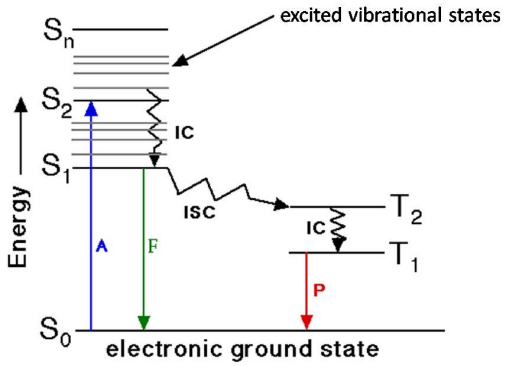

Figure 2.1: Jablonsky diagram

The fluorophore is excited from the ground singlet state, S0, to the singlet state, S1, when it absorbs a photon with an energy equal to the energy gap

ΔE between the two states. So, the frequency of the radiation light must satisfy the following condition:

$$\Delta E = h\nu$$

where h is the Planck constant (h=4.1357 10^{-15} eV s).

Absorption occurs in about 10^{-15}s, that is, much faster than nuclear motions. Consequently, nuclear coordinates do not change and the absorption process can be represented with a vertical line, as in figure 2.2.

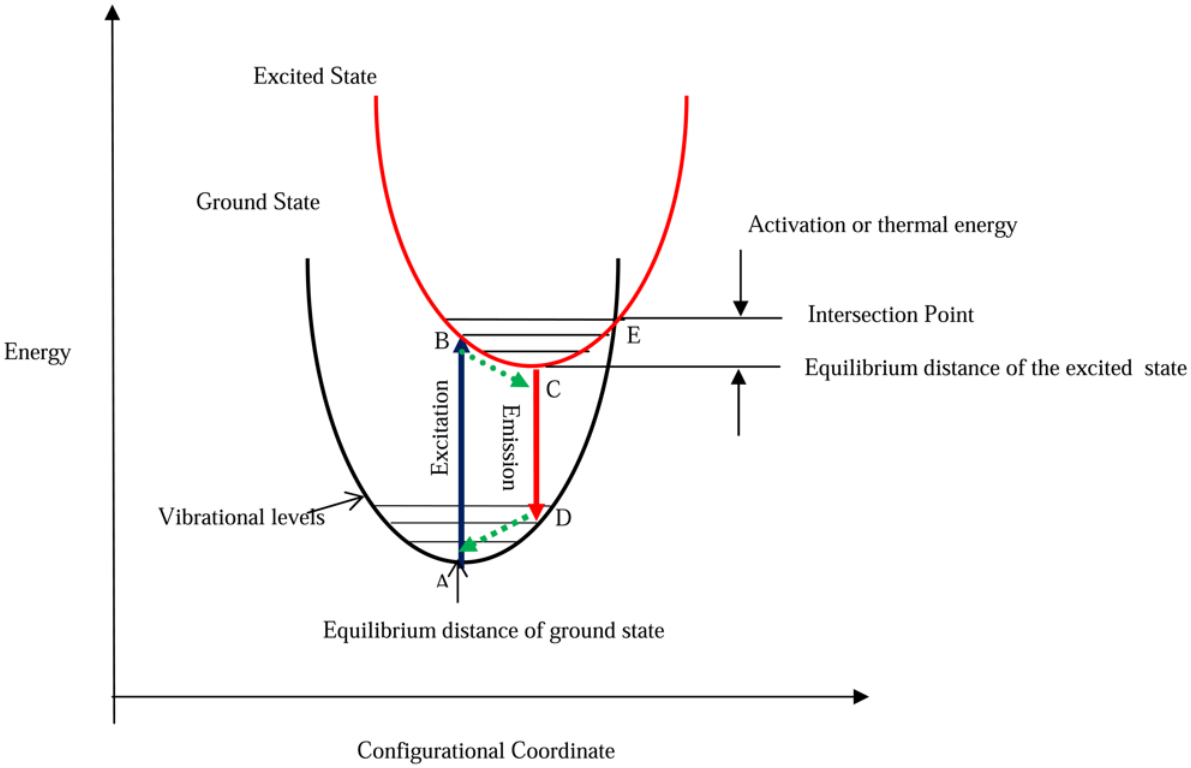

Figure 2.2: Diagram of the Frank Condon Principle

Once the fluorophore is in the excited state, it relaxes to the lowest vibrational state via internal conversion (a non radiative process that occurs faster than fluorescence; 10^{-12}s), and then relaxes to the ground state. The relaxation from S1 to S0 can occur through fluorescence emission, with lifetimes about $10^{-7} - 10^{-9}$s, or through a non-radiative de-excitation process. Consequently, fluorescence emission always occurs from the lower vibrational level of the excited singlet state, therefore, it is independent from the excitation energy (Kasha's rule). Moreover, the emission energy is lower (longer wavelength) than that of the absorption, because of the energy dissipation

caused by vibrational relaxation. This leads to a shift between the absorption and the emission spectra (Stokes‘s shift). However, absorption and emission involve the same energy levels, so the absorption and emission spectra must be symmetric to each other (mirror rule).

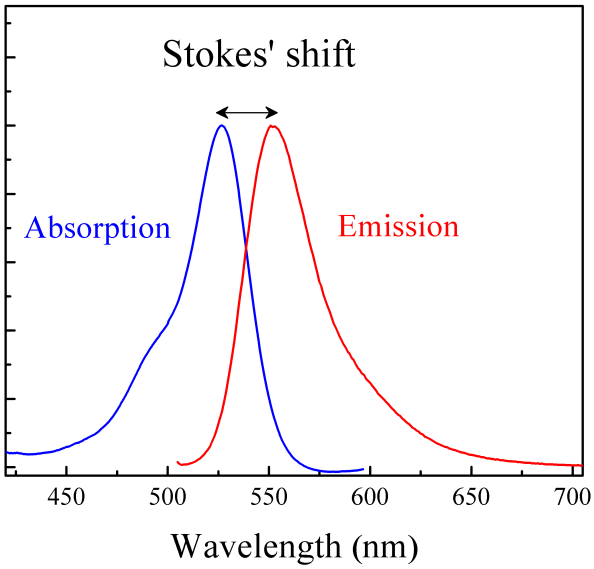

Figure 2.3: Shift between the absorption and emission spectra of a fluorophore

2.1.2 Lifetime and Quantum yield

A quantum yield, Φ, determines the brightness of the fluorophore. Considering the radiative, κ_r, and non-radiative, κ_{nr}, emission rates the quatum yield is given by the following expression:

$$\Phi = \frac{\kappa_r}{\kappa_r + \kappa_{nr}}$$

From the expression it can be seen that for the case in which most of the emission occurs in a radiative way, Φ approaches unity.

Fluorescence lifetime is defined as the average time that the fluorophore spends in the excited state before relaxing to the ground state. This can be also expressed using the previously mentioned radiative and non-radiative emission rates:

$$\tau = \frac{1}{\kappa_r + \kappa_{nr}}$$

Then, the quantum yield can be expressed as

$$\Phi = \kappa_r \tau$$

2.2 Fluorescence Correlation Spectroscopy

Fluorescence correlation spectroscopy (FCS) is a technique developed in the 70's by Magde, Elson and Webb, and it has been widely exploited to study, for example, translational and rotational diffusion and photophysical and photochemical reactions. It is based on the detection of fluctuations in the intensity of the signal emitted by the fluorophores in the excitation volume determined by a focused laser beam. By computing the temporal correlation function of those fluctuations it is possible to get information about the underlying physical processes.

2.2.1 Autocorrelation function

The fluctuations of the intensity of the signal are analyzed by the correlation function G(τ):

$$G(\tau) = \frac{\left\langle \delta F(t) \delta F(t+\tau) \right\rangle}{\left\langle F(t) \right\rangle^2}$$

F(t) is the intensity measured at time t, and τ is the delay time between two measurements. If fluorescence intensity fluctuations are slow compared to τ then F(t) and F(t+τ) will have similar magnitude and, consequently, positive values of G(τ) will result; if the fluctuations are much faster than τ the two values will be unrelated, the average of their product will be zero and so will G(τ). Therefore, the evolution of the correlation function provides information about the time scales of the processes that are responsible of the fluctuations. The term δ F(τ) represents the fluctuations of the intensity from the mean value $\left\langle F(t) \right\rangle$, so

$$\delta F(t) = F(t) - \left\langle F(t) \right\rangle$$

The explicit expression of FCS autocorrelation function depends on the geometry of the excitation volume and on the physical and chemical processes producing fluorescence fluctuations. We do not focus on autocorrelation, which will not be exploited in the present case; we describe instead cross correlation based measurements, that provides better observation for the case of a flow determining intensity fluctuations for different excitation volumes.

2.2.2 Cross-correlation function in the presence of drift motions

In the cross correlation approach FCS exploits the fluctuations of the signals gathered in two different excitation volumes located along the flow direction and at a well defined separation distance. In order to do that, the laser beam is split and focused at two different positions of the pathway of the flow. So the particles are firstly excited when they cross the first volume, and then when they cross the second; this is shown in figure 2.4.

When considering two excitation volumes, to measure the flow speed of the fluorophores, the following expression is considered:

$$G(\tau) = \frac{\langle \delta F_1(t) \delta F_2(t+\tau) \rangle}{\langle F_1(t) \rangle \langle F_2(t+\tau) \rangle}$$

where F_1 and F_2 are the signal intensities from the first and second excitation volume measured in a time t and t+τ, and τ is the delay time.

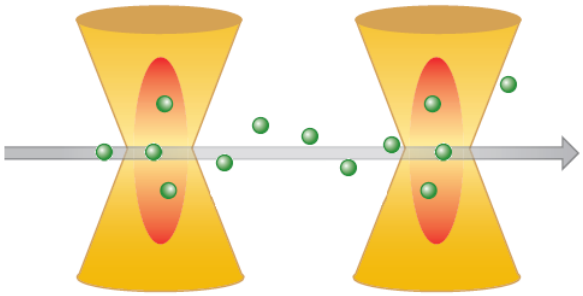

Figure 2.4: Scheme of the cross correlation setup.

Therefore, with this expression of the cross correlation function, the similarities of the two detected signal intensities coming from the two selected volumes are evaluated.

Analytically the cross correlation function depends on the geometry of the excitation volume, on the interspot distance and on the diffusive and flow properties of the detected particles:

$$G(\tau) = G(0) \frac{1}{1+\frac{\tau}{\tau_D}} \frac{1}{\sqrt{1+(\frac{\omega_0}{z_R})^2 \frac{\tau}{\tau_D}}} exp\left[-\frac{(\frac{\mathbf{R}-\tau \mathbf{v_d rift}}{\omega_0})^2}{1+\frac{\tau}{\tau_D}} \right]$$

where ω_0 is the beam waist, and z_R is the beam waist along the optical axis,

and the diffusion time τ_D is given by

$$\tau_D = \frac{\omega_0^2}{4D}$$

where D is the diffusion coefficient:

$$D = \frac{\kappa_B T}{6\pi\eta r}$$

where r is the radius of the fluorophore, η the viscosity, and T the temperature.

G(τ) is the product of a nearly hyperbolic term (defining the contribution of Brownian diffusion) modulated by an exponential factor accounting for the flow and diffusion contributions.

The weight of the diffusion term has been neglected and therefore, the flow direction has been assumed to be parallel the vector **R** connecting the centers of the excitation volumes.

In figure 2.5 an exemplary simulated cross correlation is shown. Under the assumption of a negligible diffusion coefficient the position along the lag time axis of the correlation peak is related to the time it takes on average for flowing objects to travel the distance between the two volumes. Consequently, the measurement of the blood speed is straightforward, given by the following relation:

$$v_{drift} = \frac{R}{\tau_{peak}}$$

2.2.3 Scanning Laser Image Correlation

Scanning laser image correlation (SLIC) combines laser scanning of a linear pattern with cross-correlation between any two points in the pattern providing accurate values of the direction and velocity of the flow.

In SLIC the laser beam follows a linear trajectory along the channel illuminating the excitation volumes defined by the laser beam waist. The intensity of light detected for every position of the beam is recorded. Scanning the linear path multiple times a two dimensional plot is obtained, where the x axis gives the position and the y axis the sequence of scans, that is, the time. Therefore, an xt image is obtained. Moving particles describe diagonal lines whose slope is related to the velocity and so changing slopes mean changing velocity values. A vertical line represents an immobile particle, which has the same position for all the times whereas horizontal lines are produced by molecules that move too fast comparing to the scanning

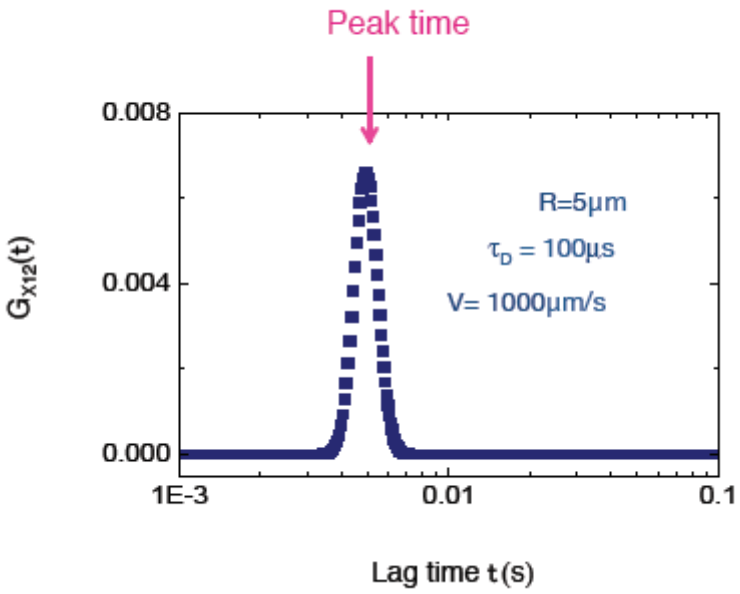

Figure 2.5: Simulated cross correlation function for R=5μm, τ_D=100μs, and $v_{drift} = 1000\frac{\mu m}{s}$.

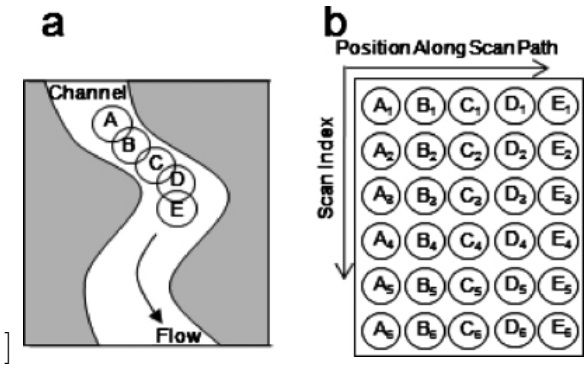

Figure 2.6: SLIC principle.

speed. Calculating the cross correlation between two columns of the image it is possible to obtain, from the peak of the function, the average time of flight that the particles need to travel the distance between the two chosen columns, and consequently the speed. In figure 2.7 two *xt images* acquired in the main vessels of the zebrafish are represented . The slope variations in the artery are due to the diastole and systolic phases, as described in the next chapter.

An important advantage of FCS is that wide spatial and temporal ranges can be considered. By setting different scanning frequencies, and hence different time length to obtain an image, a wide range of velocities can be determined, ranging from slow diffusion to fast particle flow through a channel. An appropriate image is the one that shows diagonal lines - obtained by using a scanning frequency that is higher than the flow speed of the particles. So higher values of the scanning frequency are needed as the velocity of the molecules increases. As can be seen in figure 2.7, SLIC is able to distinguish particles that travel with different velocities, which are represented as lines with different slope in the *xt carpet*.

Figure 2.7: Example of xt images for a vein in the left, and artery in the right

2.3 Experimental Setup

In FCS it is necessary to consider the smallest excitation volume possible so that to be able to distinguish the fluctuations of the intensity signal. This is possible using confocal microscopy, a technique that enables having images with high spatial resolution and low background noise.

In confocal microscopy a laser beam is focused by the microscope objective in the sample: the emitted fluorescence signal is collected by the objective in epifluorescence geometry, separated from the excitation radiation by a dichroic mirror and detected by a photomultiplier tube.

The key element of the confocal microscopy is a pinhole positioned in front of the detector, allowing the rejection of out of focus radiation. Hence, contribution of secondary fluorescence coming from out of focus planes is eliminated, leading to a background signal decrease.

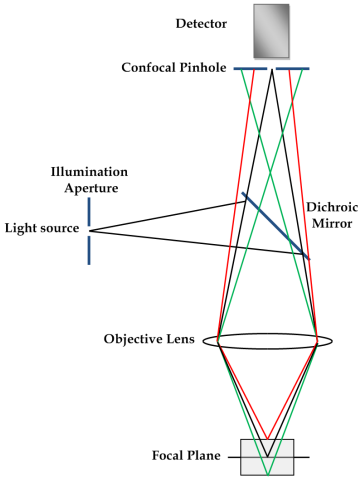

Figure 2.8: Scheme of a confocal microscope

Using a photomultiplier the detected signal intensity is amplified, and the electric signal is digitalized and sent to a computer that constructs the image by identifying each intensity signal with the related pixel.

The resolution is limited by the numerical aperture of the objective (NA), which determines the light-gathering ability, and by the excitation wavelength of the laser beam. Taking images from different planes, it is possible to construct a three dimensional image of the sample, so confocal microscopy is very useful useful when analyzing three dimensional thick organisms.

The experimental setup that has been employed consists in Leica TCS STED CW microscope, a confocal system which combines high resolution with the possibility of exploiting a wide range of scan speeds: a conventional scanner whose range is 400-1400 Hz is combined with a resonant scanner allowing the image acquisition with a 8 KHz scan frequency per each line.

Fluorescence excitation has been primed in the present work by a 561 nm laser beam.

Chapter 3

The zebrafish as a model organism

The correlation methods that have been described can be used with biological samples to obtain useful information in the fields of medicine and biology.

In this thesis work, I have centered on the hemodynamics of the zebrafish embryos, and their cardiovascular system has been studied. Organisms containing different morpholino concentration have been used, and the blood flow velocities both in the vein and arteries have been measured. As this substance slows the heart beating, a decrease in the blow velocity has been observed, and its relation with the morpholino concentration has been analysed.

3.1 Zebrafish embryos

Zebrafish embryos are widely used as animal models to study the development and functioning of the cardiovascular system, so that knowledge about cardiovascular pathologies and neovascularization processes in tumor angiogenesis is obtained. In fact, it is an ideal model organism in cancer research due to the fact that it can develop xenografts human tumor models. Therefore, comparing healthy organisms with organisms expressing pathologies the tumor vascularization processes can be better understood.

Moreover, thanks to its transparency, the zebrafish gives the possibility to visualize its internal morphology, so the vascular geometry can be easily seen.

3.1.1 Characteristics

An important advantage of the zebrafish embryos is that is possible to encode fluorescent proteins in their DNA, which allows fluorescent imaging and so FCS can be used to study hemodynamic processes. In my case, the specimen were genetically modified to express a red fluorescent protein, DS-Red, in their blood cells. So, the images have been obtained by exciting the embryos at 561 nm (absorption wavelength of DS-Red), and the emission has been collected at a wavelength about 600 nm.

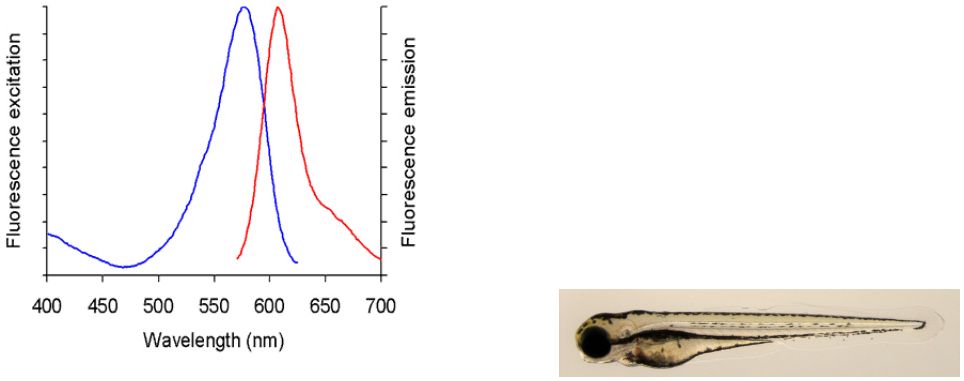

(a) (b)

Figure 3.1: a) Absorption spectrum (blue) and emission spectrum (red) of the DS-Red b) An image of the zebrafish embryo

3.1.2 Preparation of the sample

In order to observe the organism, it is necessary to have it immobilized. This has been done by using a 0.1% agarose, a polysaccharide polymer that melts in water solution at near boiling temperatures but jellies at room temperature. Specimens were thus placed into a custom-built glass chamber and immobilized in the agarose gel. As some oxygen enters in the gel, the embryo can survive for some days, so study in-vivo can be done.

Chapter 4

Analysis

This chapter is devoted to the investigation of the blood flow speed in the main vessels - namely the dorsal aorta and the post cardinal vein- of the circulatory system of (two days post fertilization) Zebrafish embryos in both healthy and pathological conditions. Alterations in both the modulus of the blood flow velocity and in the heart beat have been induced by injections, at increasing concentration, of the morpholino for the Troponine T protein, which regulates the heart contraction: by inhibiting the Troponine T expression, injections remarkably alter the cardiac activity of the embryo. Therefore, the comparison of the blood flow speed and of the heart beat frequency detected in healthy embryos and pathological ones allows assessing both the effect of a deficiency in the protein expression and the sensitivity and suitability of the SLIC technique for *in vivo* blood flow.

Each specimen has been studied by SLIC analysis: the scan line has been placed parallel to the flow at the vessel centerline, where the flux of cells passing through is the maximum; since a scan speed higher than the speed of flowing objects is required in the SLIC method a 8 KHz scan frequency has been adopted for blood flow measurements in both the vein and the artery.

4.1 Healthy embryo

First of all, a healthy embryo has been analyzed in order to be able to compare standard values obatined in physiological conditions with those obtained from the analysis of unhealthy embryos.

For each *xt image*, acquired either in the post cardinal vein or in the dorsal aorta, cross correlation functions have been computed for increasing column distances in the range 10 - 90 pixels (corresponding to 2.2 - 19.8 μm, for a typical pixel size of 0.22 μm).

Figure 4.1: Example of a xt image of the vein of a healthy embryo

.

In the simpler case of the venous vessel, the speed of the Red Blood Cells (RBCs) is approximately constant in time: hence, as reported in figure 4.1, the obtained *xt images* show parallel diagonal lines. Cross correlation functions (figure 4.2) exhibit a single peak that, as previously discussed, is directly related to the time it takes for flowing objects to travel the distance between the selected columns. By plotting the position, along the lag time axis, of the correlation peak versus the column distance, the expected linear trend is retrieved (an example is shown in figure 4.3):

$$\tau_{peak} = \frac{R}{v_{drft}}$$

where τ_{peak} is the peak time, v_{drift} the velocity and R the distance between the columns.

The speed of the blood cells can be obtained by calculating the inverse of the slope obtained from the linear fit of the graph in figure 4.3.

The analysis has been repeated on five *xt images* leading to an estimate of the average speed :

$$v = (1090 \pm 84)\frac{\mu m}{s}$$

The standard deviation reported for the five measurements reflects the physiological temporal fluctuations exhibited by blood flow speed on a living

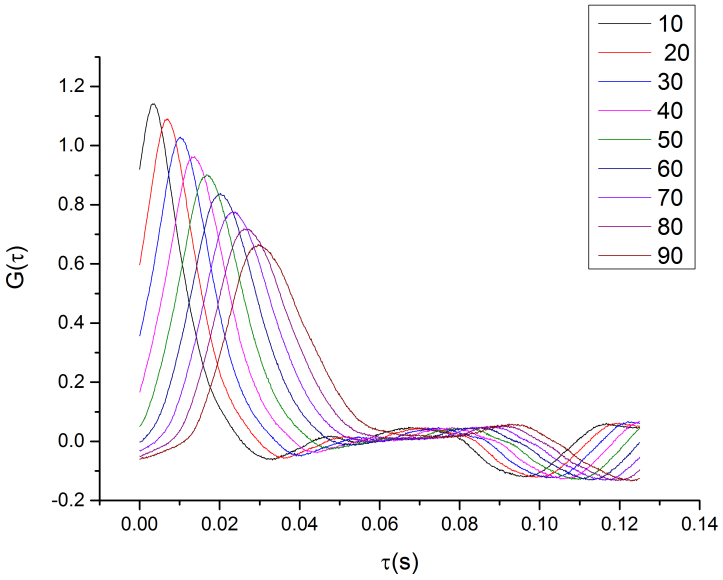

Figure 4.2: Example of cross correlation functions for the vein.

organism.

In the more complex case of the artery, blood flow inside the dorsal aorta is promoted by periodic ventricular contractions and relaxations of the heart reflected in a periodic change in the velocity: diastolic and systolic phases (*xt image* represented in figure 4.4). The image has been subdivided in various regions to be separately analyzed, obtaining different correlation functions to each region, and hence to their corresponding speed values. The slope of the diagonal lines increases during the diastolic phase (slower speed), and decreases during the systolic phase (higher speed).

Consequently, two different velocities have been obtained when studying the cross correlation functions related to the case of the artery. In figure 4.5 two examples of the obtained cross correlation function are represented. As a consequence, the peak times of the correlation functions are smaller in the systolic case (figure 4.5).

By plotting τ_{peak} versus the corresponding distances employed for the cross correlations the speed of the particles can be determined (figure 4.6). Considering a position near the heart and a central region of the vessel, where the cells move faster, the obtained values for the speed of the systolic and diastolic cardiac phases are the following:

$$v_S = (582 \pm 100)\frac{\mu m}{s} \qquad v_D = (2031 \pm 132)\frac{\mu m}{s}$$

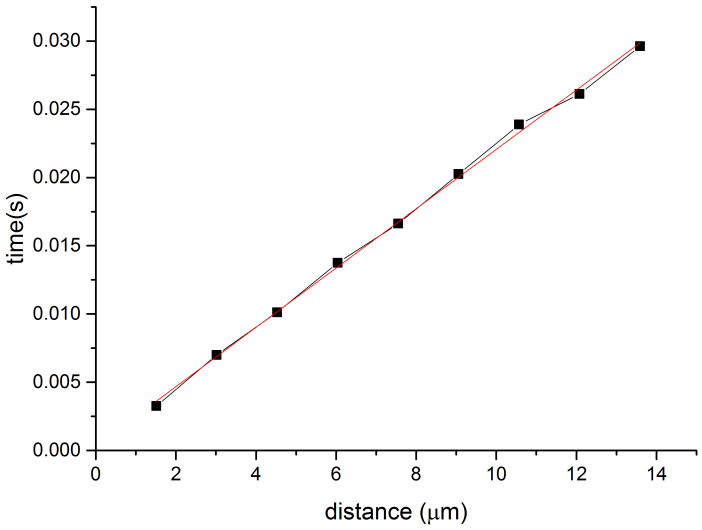

Figure 4.3: Example of the determination of the velocity through a linear fit where the inverse of the slope gives the velocity 1029 $\pm$ 6 $\frac{\mu m}{s}$. The error is equal to 0.5 $\frac{1}{\tau_{line}}$, so the length of the error bars is too small to be seen in the graph.

The velocity profile over time can be obtained with the following procedure: every carpet is divided into several regions of 256 lines each corresponding to a time interval of 32 ms and cross correlation analysis at different column distances is performed on every region to determine the average velocity of the blood cells in that time interval. This acquisition method provides higher accuracy because it is based on the idea of sectioning the carpet and a more detailed analysis is performed. The obtained velocity profile is shown in figure 4.7.

The determined periodic profile is consistent with the cardiac cycle: the blood cells speed rapidly increases to a maximum value for the systolic phase and then decreases to a minimum for the diastolic phase. From the graph the pulsation frequency is found to be three pulsations every second.

To investigate the variations of the mean velocity along the main vessels several positions from the heart to the tail have been considered to study the blood flow both in the vein and in the artery.

Figure 4.8 illustrates the velocity trend of the blood in the dorsal aorta and in the posterior cardinal vein. The analyzed specimen is characterized by a high arterial velocity in the systolic phase, an intermediate venous velocity

Figure 4.4: Example of a subdivision in the xt image for the systolic and diastolic cardiac phases. The length of the image is ~ 100 μm

.

and a slower diastolic velocity. These results agree with several measurements previously performed in the laboratory and with the literature. Several specimens had been previously investigated in the laboratory and it was found that in a region near the heart the speed of the blood cells was higher than the speed of those that where measured in a further region. In fact, the contraction and relaxation of the heart has a greater effect in its proximities than in further regions located near the tail, and this effect is shown in the variation of the velocity.

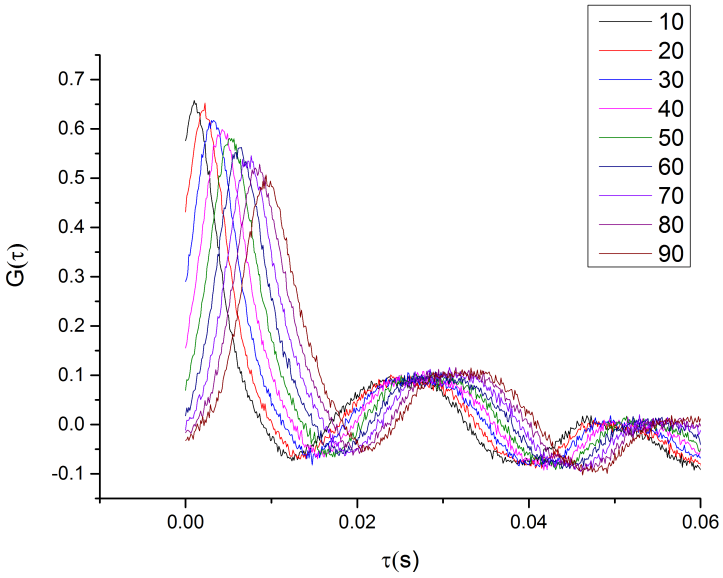

(a) Systole.

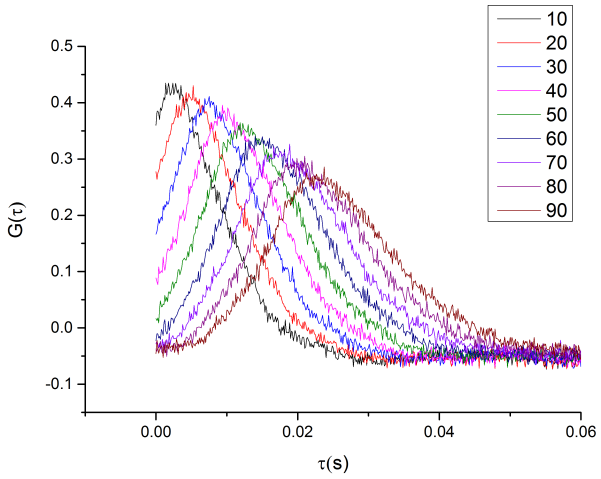

(b) Diastole.

Figure 4.5: Examples of the cross correlation functions for the systolic and diastolic cardiac phases.

4.2 Analysis for different concentrations of morpholino

The procedure to determine the speed of the blood flow has been the same as the previously explained.

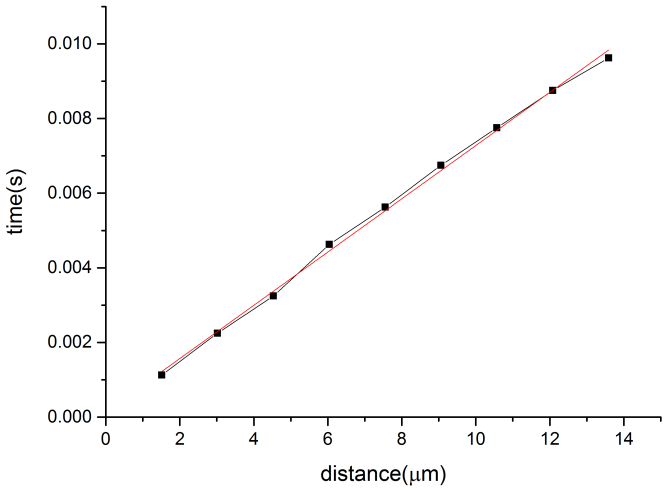

(a) Systole.

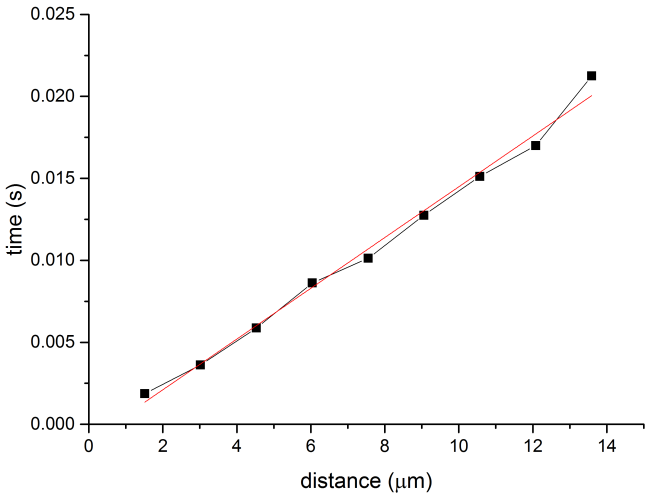

(b) Diastole.

Figure 4.6: The cross correlation peak time is reported for increasing column distance. The best linear fit is reported and also in this case the length of the error bars is too small to be seen in the graph.

In the cases of unhealthy embryos, as the morpholino leads to a lower expression of Troponina T protein, heart contractions are weaker, therefore, slower blood cells are expected. In fact, weaker contractions lead to a situa-

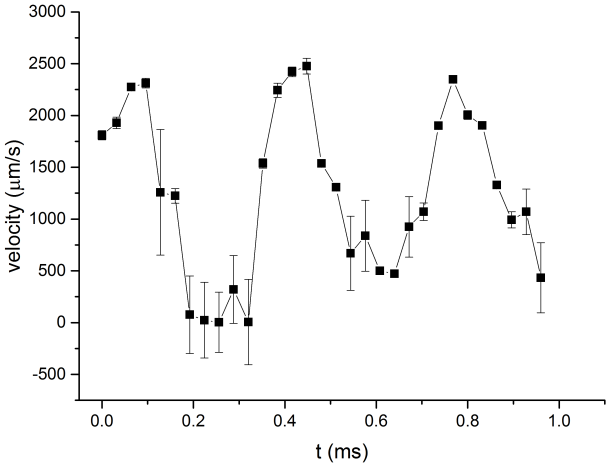

Figure 4.7: The velocity profile for a length of time of 1ms is reported for the dorsal aorta. The three peaks correspond to the maximum speed of the blood flow during the systolic phase.

tion of lower pressure to push the blood and, consequently, a lower velocity. In the analyzed xt images (figure 4.10) this can be seen due to the presence of more lines with increasing slope. Moreover, the reduction of the quantity of measured lines represents the fact that the number of red blood cells passing through the scan path per second has decreased.

In the graphic in figure 4.10 a comparison of the blood flow speed values recovered for unhealthy morpholino concentration is reported. It has been found that for all the cases in which morpholino has been injected the measured speed value has decreased both in the artery and the vein.

The cardiac cycle refers to a complete heartbeat from its generation to the beginning of the next beat, and so includes the diastole and the systole. The frequency of the cardiac cycle is described by the heart rate and each beat is determined by the contraction and relaxation of the heart. Consequently, for a specimen with high concentration of morphorline its value is smaller than for a healthy specimen, or one with a lower concentration (figure 4.11).

Comparing those graphs with the ones obtained for the case of the healthy specimen, a remarkably change in the pulsation frequency has been observed: in the case of the healthy embryo three pulsations have been found (see figure 4.7) frequency, instead of three pulsations two have been determined. Therefore, it has been computed that more time is needed to complete the cardiac cycle. The value of the reached maximum velocity has been significantly

reduced. Apart from that, the two pulsations are not so well defined as in the case of the healthy embryo because of the reduced quantity of blood cells that has been analyzed.

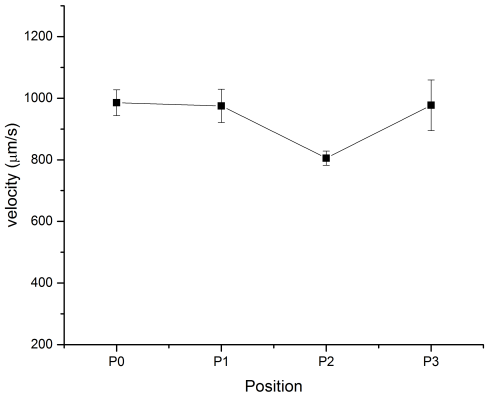

(a) Vein

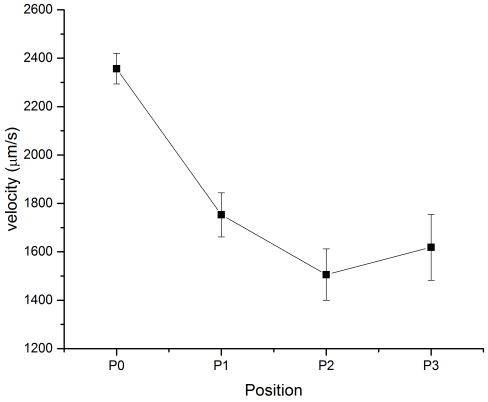

(b) Systole

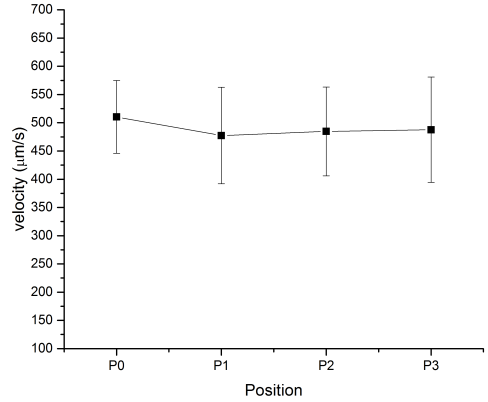

(c) Diastole

Figure 4.8: Variation of the velocity for different positions along the main vessels. The positions P0, P1, P2 and P3 correspond to increasing distances from the heart (P0) to the tail (P3) at $\sim 300\mu$m separation.

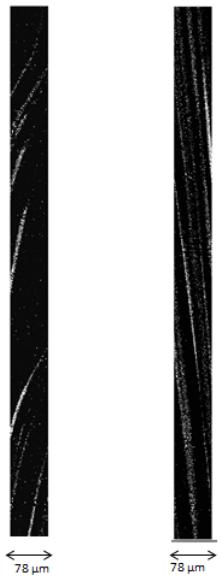

Figure 4.9: The two images are examples of xt images obtained for the vein and artery in the case of a morpholine concentration of 0.02pmol/embryo. In the vein the obtained lines are almost vertical and in both cases the number of lines is slower than in the case of the healthy embryo.

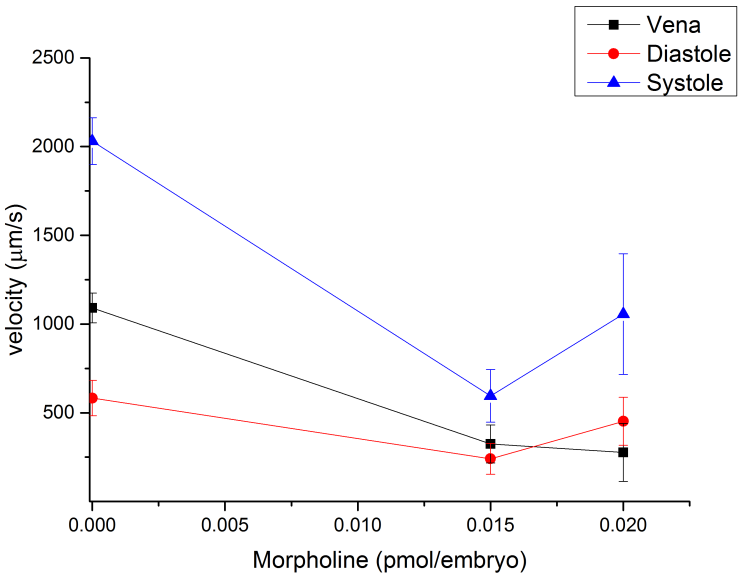

Figure 4.10: Variation of the speed for different morpholine concentrations.

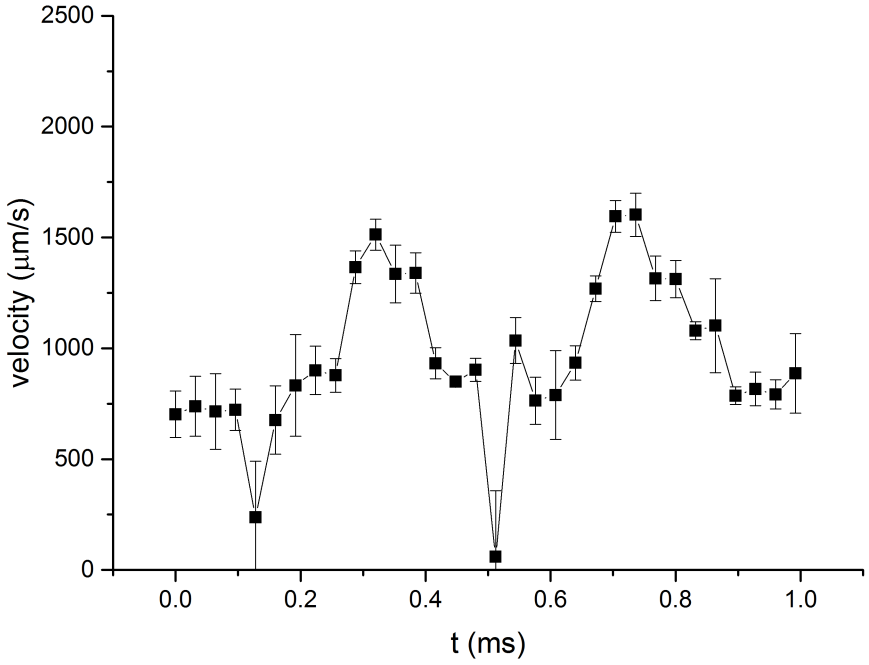

(a) Embryo with a concentration of morpholino 0.02pmol

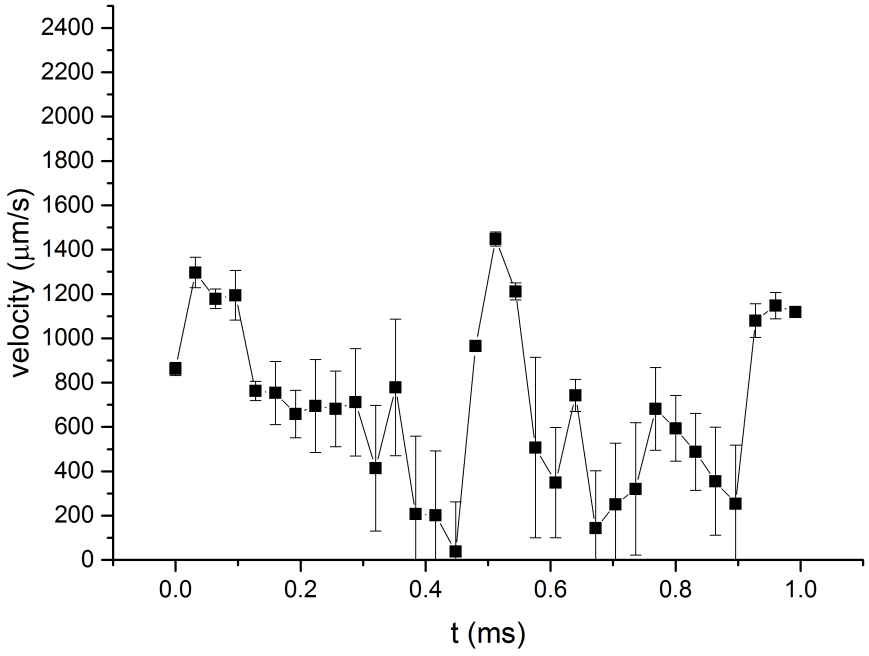

(b) Embryo with a concentration of morpholino 0.015pmol

Figure 4.11: Velocity profile in the dorsal aorta. The maximum speed values reached in the systolic phase are represented by the two peaks.

Chapter 5

Conclusions

The aim of the thesis work has been to investigate flow dynamics inside a living organism by using SLIC method, hence learning the basics and applications of confocal microscopy and fluorescence correlation spectroscopy in the field of biophysics. The topic of investigation of in vivo flow dynamics, blood flow in living organisms, provides the possibility to investigate a wide range of cardiovascular pathologies. In this particular case, the effect of a deficit of Troponine T protein has been analyzed, and it has been observed that people presenting weak heart throb does have low concentration of this protein. Therefore, analyzing its effect and behavior in the circulatory system, having a medical background, heart pathologies could be prevented.

Consequently, the characterization of the circulatory system of zebrafish embryos can be used in comparative studies between healthy organisms and embryos affected by specific pathologies. In particular an important clinical application is the study of the early stages of tumor development and vascularization which can be performed comparing healthy embryos with embryos in which human tumor cells are transplanted.

Therefore, being able to analyze and characterize blood flow for different conditions has a great importance regarding medical investigation, and during the thesis work, SLIC has been found to be an accurate method for flow investigation in the zebrafish embryo: different results have characterized different organism conditions. Fluorescence correlation spectroscopy has shown its validity for flow measurements and the obtained low errors (almost a straight line has been represented in all the plots when doing the fit of the peak time versus the column distance) represent the accurateness of the method.

Chapter 6

Bibliography

- Michelle A.Digmann and Enrico Gratton, *Imaging Barriers to Diffusion by pair Correlation Functions*, University of California, Irvine, California (2009).
- Micheal H.Malone, Noah Sciaky, Lisa Stalheim, Klaus M. Hahn, Elwood Linney e Gary L.Johnson, *Laser-scanning velocimetry: a confocal microscopy method for quantitative measurement of cardiovascular performance in zebrafish embryos and larve*, University of North Carolina (2007).
- Molly J.Rossow, William N.Mantulin and Enrico Gratton, *Scanning laser image correlation for measurement of flow*, University of California, Irvine, California (2010).
- Margaux Bouzin, Laura Sironi, Paolo Pozzi, Laura D'Alfonso, Maddalena Collini and Giberto Chirico, *Fluorescence cross-correlation for in-vivo hemodynamics measurements - Abstract* -, Physics Department, University of Milano Bicocca, Milano (2014).
- Valeria Chiara Mauri, *Image correlation spectroscopy to investigate hemodynamics - Master degree thesis* -, Physics Department, University of Milano Bicocca, Milano (2013).
- S.Inouè, *Foundation of confocal scanned imaging in light microscopy.*

Chapter 7

Ringraziamenti

Vorrei ringraziare la professoressa Maddalena Collini per averme proposto questo stage, e per la sua disponibilitá e pazienza. La dottoressa Margaux Bouzin per l´immensa pazienza, per avermi aiutata tantissimo. Grazie in particolare a Nicolò, per i suei consigli e infinita disponibilitá. A Cassia, per tutto iil suo aiuto.
In generale, grazie a tutti del dipartimento di biofisica.
Soppratutto non ho parole per ringraziare i compagni di laboratorio, il suo aiuto è stato meraviglioso.
Grazie a tutti.